EuroIntervention

Design principles and performance of bioresorbable polymeric vascular scaffolds

James P. Oberhauser, PhD; Syed Hossainy, PhD; Richard J. Rapoza, PhD

Abbott Vascular, Santa Clara, CA, USA

All authors are employees of Abbott Vascular.

KEYWORDS
Bioresorbable vascular scaffold, vascular restoration therapy, percutaneous coronary intervention, stent, coronary artery disease, vasomotion

Abstract

Aims: Bioresorbable polymeric vascular scaffolds may spawn a fourth revolution in percutaneous coronary intervention (PCI) and a novel treatment termed vascular restoration therapy. The principal design considerations for bioresorbable scaffolds are discussed in the context of physiological behaviour using the Bioabsorbable Vascular Solutions (BVS) ABSORB Cohort B scaffold (Abbott Vascular) as an example.

Methods and results: The lifecycle of a bioresorbable scaffold is divided into three phases: (1) revascularisation; (2) restoration; and (3) resorption. In the revascularisation phase spanning the first three months after intervention, the bioresorbable scaffold should perform comparably to metallic drug-eluting stents (DES) in terms of deliverability, radial strength, recoil, and neointimal thickening. The ensuing restoration phase is characterised by gradual erosion of radial strength and a loss of structural continuity, where the time scale at which each occurs is related to the hydrolytic degradation rate of the polymer. Natural vasomotion in response to external stimuli is theoretically possible at the end of this phase. Finally, in the resorption phase, the passive implant is systematically resorbed and processed by the body.

Conclusions: Limited clinical data speak to the potential of bioresorbable scaffolds as a new therapy, and future studies will prove critical to inspiring a fourth revolution in PCI.

** Corresponding author: Abbott Vascular, 3200 Lakeside Drive, Santa Clara, CA 95054, USA*
E-mail: james.oberhauser@av.abbott.com

Introduction

Percutaneous coronary intervention (PCI) as a treatment for atherosclerosis has experienced three revolutions in treatment strategy. The first came in the form of balloon angioplasty, which showed success in opening occluded vessels but was prone to early elastic recoil and constrictive remodeling.[1,2] Both phenomena were rectified by the second revolution, bare-metal stents (BMS), although a new problem arose in the form of excessive neointimal growth that contributed to restenosis. Moreover, unlike balloon angioplasty which offered no vessel scaffolding, BMS permanently scaffolded the vessel, frequently limiting reintervention at the same site, if necessary, to coronary artery bypass graft (CABG) surgery. The third revolution, drug-eluting stents (DES), largely solved the problem of excessive neointimal growth through the addition of antiproliferative agents coated on the surface of stents. However, DES led to a new but infrequent problem of late stent thrombosis, likely due to the delayed formation of cellular matrix and functional endothelium over stent struts.[3-5] DES also permanently scaffold the vessel like BMS.

Bioresorbable stents have been suggested as a possible fourth revolution in PCI.[6] The central thesis is that vessel scaffolding is only required transiently, and therapeutic benefit may be derived from allowing natural vasomotor response in the vessel. Other potential benefits include reduced or eliminated late stent thrombosis and facilitated reintervention due to the complete resorption of the implant, improved non-invasive imaging of the target site during post-intervention follow-up using computed tomography or magnetic resonance, and shorter prescription of dual anti-platelet therapy. Limited clinical data from the Igaki-Tamai bioresorbable stent[7] (Kyoto Medical Planning Co., Ltd., Kyoto, Japan) and the Bioabsorbable Vascular Solutions (BVS) bioresorbable stent[8,9] (Abbott Vascular, Santa Clara, CA, USA) offer promising signs, but more clinical study across a broader range of patient histories and disease states is necessary before a fourth revolution may be proclaimed.

Nevertheless, the ability to restore natural vascular response is the feature that distinguishes bioresorbable stents from BMS and DES and spawned a novel therapeutic description, vascular restoration therapy (VRT). While the benefits of VRT remain to be proven clinically, vasomotion and endothelial function are central to the discussion. A healthy, functioning endothelial layer controls thrombosis and thrombolysis, platelet and leukocyte interactions, the release of vasodilating (e.g., nitric oxide) and vasoconstricting (e.g., endothelin-1) substances, and generally regulates vascular tone and growth.[10,11] On the other hand, the relationship between endothelial dysfunction and atherosclerosis is well known, predisposing the vessel to vasoconstriction.[12,13] Fortunately, endothelial dysfunction has been shown to be reversible.[14] For instance, exercise training has been shown to improve endothelium-dependent vasodilation in patients with coronary artery disease, suggesting that vasomotion and endothelial function may be related.[15]

For natural vascular response to return to a treated vessel, a bioresorbable stent must cease scaffolding the vessel at some point after intervention. Essentially, it must lose radial strength and structural continuity and no longer function as a stent. The fact that the term stent implies permanence renders the phrase bioresorbable stent oxymoronic. Thus, throughout this article, the term scaffold, which is more suggestive of a temporary structural element, will replace stent in the context of bioresorbable devices.

The challenge of developing a bioresorbable polymeric coronary scaffold derives principally from its intrinsic temporary nature. Specifically, device performance (e.g., duration of radial scaffolding and structural continuity) must be aligned with physiological behaviour (e.g., lumen stabilisation, cellular matrix deposition). This treatise seeks to outline the design principles and performance attributes believed to be essential in a bioresorbable vascular scaffold. While there are undoubtedly numerous polymeric materials, scaffold designs, and resorption profiles capable of meeting these goals, the BVS ABSORB Cohort B scaffold will be used as an example.

BVS ABSORB Cohort B device

Materials

Bioresorbable polymers have been the subject of extensive scientific research and commercial development in fields as diverse as food packaging and biomedical devices. One such class of materials is polylactide (PLA), a member of the aliphatic polyester family of materials, which is attractive because it may be manufactured from renewable resources into products with mechanical properties similar to those associated with commodity polymers such as polyethylene, polypropylene, and polystyrene. Polylactide polymers and copolymers containing lactide or lactic acid have a long history of use in medical devices starting with bioresorbable sutures in the 1960s. These polymers are now used in a wide range of bioresorbable implants, including: orthopaedic devices, such as plates, pins and screws; drug delivery systems such as solid implants and gel based systems; suture anchors; and surgical mesh and clips.

The BVS ABSORB Cohort B device consists of a poly(L-lactide) (PLLA) scaffold, a coating layer of poly(D,L-lactide) (PDLLA) and the antiproliferative drug everolimus, a pair of radiopaque markers at the proximal and distal ends of the scaffold, and a balloon catheter delivery system. An image of the scaffold is shown in Figure 1. PLLA is a semicrystalline polymer whose degree of crystallinity and crystalline microstructure are dependent upon the thermal and deformation history during processing. The high tensile strength and modulus of PLLA make it suitable for load bearing applications. PLLA has a maximum crystallinity of approximately 70%, a melting temperature (T_m) of 175-180°C, and a glass transition temperature (T_g) of 55-65°C.

Because it is a random copolymer derived from an equimolar mixture of D- and L-lactide, PDLLA is incapable of forming crystalline structure and, hence, is fully amorphous. Consequently, this material is characterised by a lower tensile strength and higher elongation at break than PLLA. Because amorphous polymers lack crystalline structure, they do not have melting temperatures but instead begin to flow at temperatures in excess of T_g, which for PDLLA is similar to that for PLLA when both are of sufficiently high molecular weight.

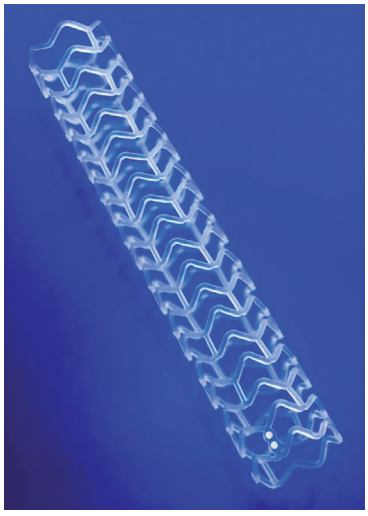

Figure 1. Image of the BVS ABSORB Cohort B 3.0 x 18 mm scaffold.

Hydrolysis of PLA

In the case of the PLA family of polymers, molecular weight degradation occurs in vivo predominantly through hydrolysis, which is a bimolecular nucleophilic substitution reaction that can be catalysed by the presence of either acids or bases. The schematic shown in Figure 2 describes the hydrolysis reaction in which water catalyses a chain scission event at an ester bond. Since each monomer subunit contains one ester bond, chain scission of any given PLA chain is equally likely to occur anywhere along the chain for a purely amorphous material.

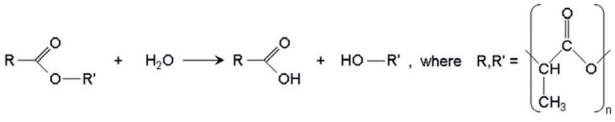

Figure 2. Reaction pathway for hydrolytic degradation of the PLA family of polymers.

For objects whose smallest dimension is O(100 μm), hydrolysis by-products cannot readily diffuse out of the object, and bulk degradation controls the process. That is, the object degrades more or less from the inside out. In this case, the generally accepted third-order kinetics theory of Pitt et al predicts that the hydrolysis rate depends upon the concentration of ester bonds, water, and carboxylic acid end groups, the latter of which are generated by each hydrolysis reaction.[16-18] This so-called autocatalytic model for aliphatic polyesters like PLA is based upon the third-order rate equation given by:

$$\frac{d[E]}{dt} = -\frac{d[COOH]}{dt} = -k[COOH][H_2O][E], \quad (1)$$

where [E], [COOH], and [H_2O] represent the concentrations of ester bonds, carboxylic acid end groups, and water, respectively, and k is the hydrolytic degradation rate constant. Assuming that the concentrations of ester bonds and water are approximately constant throughout the degradation process and the concentration of carboxylic acid end groups is inversely proportional to the number-average molecular weight (M_n) of the polymer (i.e., [COOH] = 1/M_n), Weir and co-workers[19,20] showed that:

$$M_n(t) = M_n(0)\exp(-kt), \quad (2)$$

where $M_n(t)$ is the number-average molecular weight after degradation time t, and $M_n(0)$ is the number-average molecular weight at time t=0 (prior to degradation). The assumptions inherent in the model are reasonable provided that mass loss has not occurred, since mass loss would affect the concentrations of water and carboxylic end groups in the sample. Eq. (2) may be rewritten as:

$$\ln\left(\frac{M_n(t)}{M_n(0)}\right) = -kt. \quad (3)$$

By representing data for $M_n(t)/M_n(0)$ versus t on a log-linear plot, one may infer the hydrolytic degradation rate from the slope of the line connecting the points.

The hydrolytic degradation of the PLLA scaffold governs its mechanical performance and occurs over three distinct stages. In the first stage, water diffuses into the less dense amorphous regions of the scaffold and hydrolyses ester bonds. The only observable effect at this stage is a reduction in molecular weight, as described by the hydrolytic degradation model above. Because hydrolysis is most active in the amorphous region, a slight increase in the degree of crystallinity of the device is often observed during this stage. The second stage is marked by a reduction in radial strength, caused by the scission of amorphous tie chains linking crystalline regions. At this time, cracks and structural discontinuities are normal and entirely expected, since the device is designed to degrade and be physiologically processed over time. Finally, in the third stage, polymer chains have been hydrolysed to sufficiently short lengths that they are increasingly hydrophilic (and hence, soluble in an aqueous environment) and able to diffuse out of the device and be resorbed into the body.

Phases of device performance

The introduction of a foreign body into the vasculature initiates a cascade of complex physiological responses. The initial injury invariably caused by implantation of a scaffold intended to recanalise the vessel leads sequentially to platelet deposition, leukocyte recruitment, smooth muscle cell proliferation, deposition of cellular matrix, and, hopefully, re-endothelialisation of the treated portion of the vessel. Platelet deposition and leukocyte recruitment are of particular note in light of the fact that they drive thrombosis and inflammation, respectively.

For traditional metallic DES, the relationship between physiology and device performance is relatively simple and strongly influenced by acute properties. For instance, metallic DES are typically designed to have high radial strength upon implantation that is maintained, ideally, in perpetuity. Moreover, DES elute an anti-proliferative therapeutic agent at a prescribed rate to inhibit the cellular proliferation that can lead to restenosis. It is expected that vessel healing concludes with re-endothelialisation on some time scale, but the vessel remains permanently scaffolded. Consequently, external stimuli (e.g., exercise) that would naturally tend to stimulate vessel dilation cannot have that effect.

On the other hand, bioresorbable scaffolds are subject to an entirely different set of performance criteria, due primarily to the fact that they should match the near-term performance of traditional metallic DES but resorb into the body on longer time scales. Therefore, their design requirements bear a different relationship with the physiological response, one that is qualitatively described in Figure 3.[21] Here, the lifecycle of the bioresorbable scaffold is divided into three phases: (1) revascularisation; (2) restoration; and (3) resorption. The detailed design criteria for the scaffold in each of these phases and the connection to physiological behaviour will be discussed below.

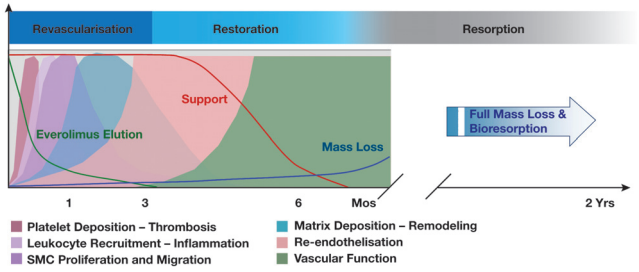

Figure 3. Conceptual representation of the three phases of bioresorbable scaffold functionality and the relationship to physiological responses following implantation.

Revascularisation phase

The revascularisation phase is that in which bioresorbable scaffolds should most closely mimic the design considerations of metallic DES. Specifically, the device should possess good deliverability to the target site, the scaffold should be deployed with a minimum of recoil and provide high acute radial strength, and the therapeutic agent should be delivered to abluminal tissue at a controlled rate. In this discussion, we will focus attention upon deliverability and radial strength, since those topics are perceived to be most challenging to device development.

Since the flexibility of a crimped scaffold is instrumental to its ability to navigate a tortuous path, it may be evaluated as a surrogate for deliverability. One test of flexibility is a three-point bend test, where the ends of the crimped scaffold are fixed and a normal force is imposed at the centre-point of the device using an Instron (Illinois Tool Works Inc., Glenview, IL, USA). The maximum compressive load required to deflect the device by 1.1 mm is one key measure of flexibility, where a lower force suggests greater flexibility. The results for both the ABSORB Cohort B device and XIENCE V stent system (both 3.0 x 18 mm devices) are presented in Figure 4. Despite the fact that the strut thickness of the ABSORB Cohort B scaffold is greater than that of XIENCE V (ca. 152.4 µm versus 81.3 µm), the maximum compressive load for the ABSORB Cohort B device is statistically significantly lower than that of XIENCE V ($p = 0.004$). In this test and in clinical practice, flexibility is strongly influenced by the scaffold pattern, scaffold material properties, and catheter flexibility. Because the catheter used in the two devices is equivalent, one may infer that the closed-cell pattern of the ABSORB Cohort B scaffold and the polymer material properties lend the device its favourable flexibility. Imbuing bioresorbable polymer scaffolds with acute radial strength comparable to that of metallic DES is perceived to be one of the most significant developmental challenges. On the surface, intrinsic polymer material properties are less impressive than those of numerous metal alloys.[22,23] However, the deformations imposed in polymer processing can drive these materials into complex morphologies with a high degree of anisotropic structure.[24,25] The resulting macroscopic properties are directly related to that microstructure. Hence, the processing history, the geometry of the test article, and the direction of mechanical testing relative to any microstructural anisotropy must be considered in reporting any polymer mechanical data. Testing of semicrystalline polymers (e.g., PLLA) is particularly sensitive to the principal orientation direction of crystallites, since mechanical testing parallel to that orientation will lead to an entirely different set of results than testing in the perpendicular direction. Unfortunately, the tables of polymer properties frequently encountered in broad subject matter texts neglect to specify these details and paint an incomplete picture of the varied properties one can access through polymer processing. In the case of an object based upon a cylindrical geometry like the scaffold, radial (or hoop) strength is derived from not simply a high degree of crystallinity but specifically crystallites preferentially oriented in the circumferential direction. Crystalline orientation is nearly always imparted through the application of a deformation above the T_g of the polymer, which drives polymer molecules into a non-equilibrium, chain-extended state. In that state, line nuclei are prolifically created, and these quickly form the primary crystallites that are resistant to normal forces.[26] The manner in which one would drive circumferential orientation of these primary crystallites is achieved similarly to that in which one would create a polyethylene terephthalate (PET) beverage bottle, namely through stretch blow molding.[27] In this case, a cylindrical preform is expanded mostly radially but also axially, imparting significant circumferential orientation of crystallites and high resistance to radial loading. The empirical evidence for the effectiveness of polymer processing at engendering high radial strength is supplied by the acute radial strength data for the ABSORB Cohort B scaffold shown in Figure 5. It is clear that the ABSORB Cohort B scaffold

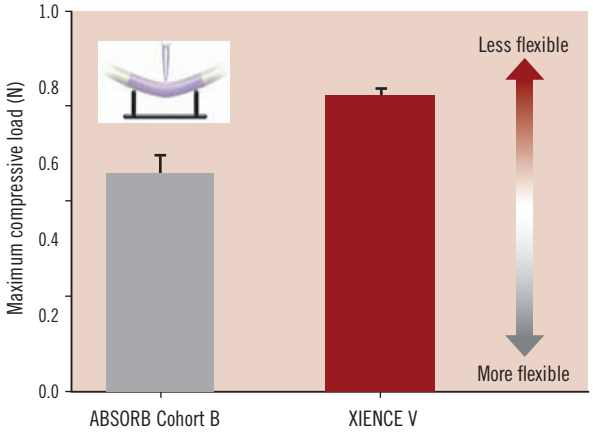

Figure 4. Maximum compressive load applied to deflect ABSORB Cohort B and XIENCE V 3.0 x 18 mm devices by 1.1 mm using three-point bend test (n = 5). Statistical analysis yielded p=0.004 using one-way ANOVA analysis and Tukey-Kramer HSD. Tests were performed by and data are on file at Abbott Vascular.

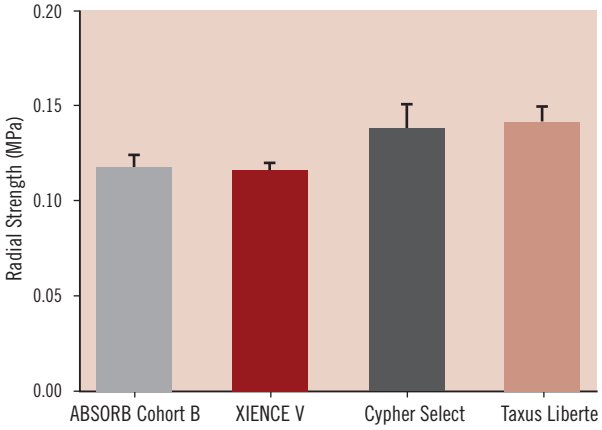

Figure 5. Acute radial strength data for ABSORB Cohort B (3.0 x18mm), XIENCE V (3.0x18 mm), Cypher Select (3.0x18 mm), and Taxus Liberté (3.0x20 mm) (n=5 for each set) obtained using the MSI RX550 radial expansion force gauge. Tests were performed by and data are on file at Abbott Vascular.

possesses a radial strength comparable to that of XIENCE V (Abbott Vascular, Santa Clara, CA, USA) and similar to that of Cypher Select (Cordis Corp., Johnson & Johnson, Warren, NJ, USA) and Taxus Liberté (Boston Scientific Corp., Natick, MA, USA).

Returning to the conceptual diagram in Figure 3, the scaffold should provide luminal support for a minimum of three months. The criticality of the three-month time point is suggested by extensive PTCA clinical data. Serruys et al[28] noted that minimal luminal diameter and percent diameter stenosis tended to stabilise after the three-month follow-up (n = 342), while Asakura et al[29] observed that neointimal thickness peaked at three months before receding out to three years (n = 30). Both studies point to lumen stabilisation approximately three months after intervention in the absence of any scaffolding. Therefore, from the standpoint of designing a bioresorbable scaffold, one may construe that erosion of radial support is acceptable after three months. However, the scaffold should be designed to maintain radial strength for at least three months despite the inevitable loss of molecular weight associated with hydrolysis. The discussion surrounding how that design objective may be achieved is reserved for the subsequent section.

Restoration phase

The restoration phase characterises the transition from active support of the lumen to a passive implant consisting of discontinuous structural elements. The aggregate of radial scaffolding and structural continuity is represented by the curve labelled "Support" in Figure 3. Significantly, when the state of structural discontinuity is reached, constriction and dilation of the vessel should no longer be inhibited by the scaffold. While vasomotion is undoubtedly strongly influenced by the specifics of the patient and the disease state, the restoration of a natural vasomotor response, unconstrained by the scaffold, is the salient feature of this phase.

The manner in which the scaffold loses radial strength is a principal design consideration. As mentioned previously, hydrolysis of ester bonds causes a reduction in polymer molecular weight until the material is reduced to its monomer subunits and physiologically processed. Immediately after intervention, water diffuses into the amorphous regions of the scaffold and begins hydrolysing ester bonds. However, significant molecular weight reduction can occur without any apparent loss in radial strength. The oriented crystallites that comprise the load-bearing structural elements are hydrolysed at their surfaces, which is a slow process. On the other hand, the amorphous tie chains that connect oriented crystalline domains are quite susceptible to hydrolysis throughout their bulk. Preservation of scaffold radial strength is governed by the lifetime of tie chains. A useful metaphor is that of a building superstructure, where girders are symbolic of the oriented crystallites and weld points of tie chains. Here, weld points are essential to joining girders into a coherent superstructure. When the weld points are removed, the superstructure can no longer hold its shape even though the individual girders remain strong. Thus, when a sufficient fraction of amorphous tie chains have been hydrolysed, the scaffold will no longer be capable of supporting a radial load.

Therefore, a direct relationship between the hydrolytic degradation rate of the scaffold polymer and the time point at which radial strength is lost should logically exist. The accuracy of this hypothesis is demonstrated in Figure 6. Here, ABSORB Cohort B scaffolds known to have varying degradation rates were placed in phosphate-buffered saline (PBS) at 37°C and pH 7.4 for prescribed periods of time and subsequently tested for either M_n or radial strength. Normalising $M_n(t)$ by $M_n(0)$ and plotting the data as a function of in vitro degradation time in Figure 6(a) reveals that the sample sets do indeed degrade at different rates. Moreover, the solid lines that represent Eq. (3) fit the data well (R^2=0.836–0.977) and support the validity of the autocatalytic hydrolysis model. Turning next to the concomitant radial strength data in Figure 6(b), it is apparent that the faster degrading samples lose radial strength at earlier time points, ratifying the hypothesis of a direct relationship between degradation rate and radial strength loss. It is also clear that a hydrolytic degradation rate consistent with that given by the green curve in Figure 6(a) meets the criterion of providing high radial strength for a minimum of three months after intervention.

Not only is the scaffold designed to lose radial strength, but it must also become structurally discontinuous still later into the degradation process as part of its natural disintegration. The location of structural discontinuities can be influenced through the balance of radial and axial strain imparted during the stretch blow moulding process. It has already been noted that circumferentially oriented crystallites induced by large radial deformations leads to high radial strength; however, pure circumferential orientation without axially oriented crystallites could render the scaffold susceptible to discontinuities along axial connector links over time. Conversely, too much emphasis on axially oriented crystallites could strengthen connectors but reduce radial strength to an undesirable level. Since high acute radial strength is a primary design requirement, radial strain and circumferential orientation of crystallites must be emphasised. The key question is the time point at which structural discontinuities, presumably at connectors, are acceptable. Referring to Figure 3, one might postulate that these discontinuities may safely occur after cellular matrix has covered

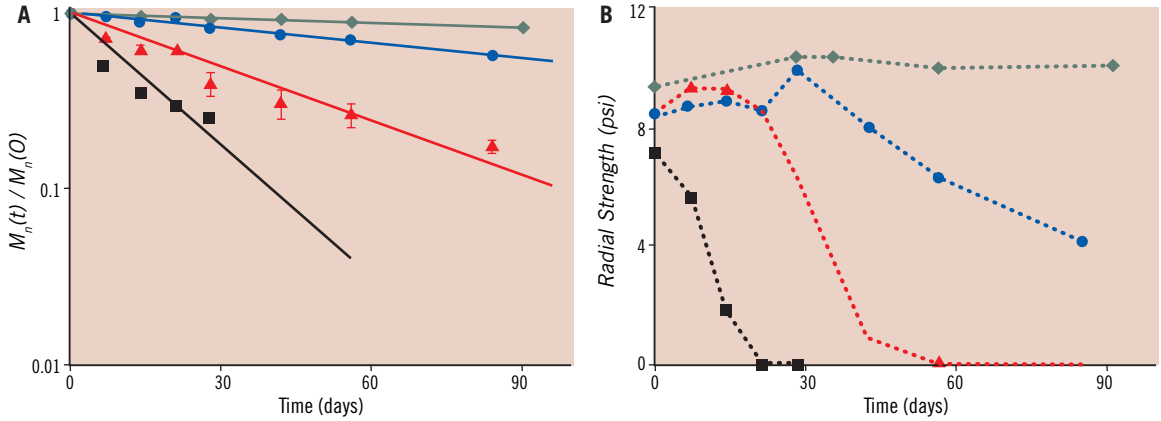

Figure 6. (a) Number-average molecular weight at various in vitro degradation times normalised by the value at t=0 [$M_n(t)/M_n(0)$] for ABSORB Cohort B scaffolds with varying hydrolytic degradation rates. Solid lines represent fits to the model given by Eq. (2). Data for Mn were obtained using gel permeation chromatography with refractive index detection. (b) Radial strength as a function of in vitro degradation time for the same lots of scaffolds as in (a). The dotted lines are intended only to aid the eye. Note that the irreversible deformation test method used to generate these data differs from that used to obtain the data in Figure 5, and the two sets of data may not be directly compared. Sample sizes vary between n=3 and n=6. Tests were performed by and data are on file at Abbott Vascular.

the surface of the scaffold, thereby fixing it in place. In the ABSORB Cohort A trial of 30 patients, a subset of 13 patients received optical coherence tomography (OCT) at the six-month time point, which showed that 664 of 671 (99%) of scaffold struts were covered with neointimal tissue.[8] While this cellular matrix may, in fact, have deposited over struts earlier than six months (the time point of the first imaging follow-up), the result suggests that a design constraint that the scaffold not be discontinuous until greater than six months after intervention is reasonable.

While it is unclear when precisely natural vasomotor response is possible, one might postulate that it is linked to the loss of radial strength and structural continuity between scaffold rings. In the context of Figure 3, when the "Support" curve approaches zero, the restoration of natural vasomotor function is theoretically possible. However, because of the probable dependence upon patient physiology and disease state, the boundary between the end of the restoration phase and the resorption phase is nebulous and treated as such in the conceptual diagram.

Resorption phase

After the scaffold becomes structurally discontinuous, it ceases to perform any scaffolding role and may be considered functionally inert. As such, in the resorption phase, the scaffold will now be referred to as an implant, which better reflects its passivity. The sole remaining design constraint on the implant is that it be resorbed in a benign fashion.

The resorption process begins with PLA being hydrolysed to lactic acid and diffusing into surrounding tissue and perhaps the bloodstream. Because the BVS ABSORB Cohort B implant is comprised of both PLLA and PDLLA polymers, the ultimate degradation products include both L-lactic acid and D-lactic acid. As acids, they are proton donors, meaning that L-lactic acid and D-lactic acid can dissociate to form L-lactate and D-lactate, respectively, plus a proton (H^+). However, the pKa of lactic acid is 3.84, making it a fairly weak acid.[30]

Moreover, L-lactate, D-lactate, and protons are biologically ubiquitous. Protons are produced and consumed constantly in physiological reactions, including hydrolysis of adenosine triphosphate (ATP) and glycolysis.[31] L-lactate is believed to participate as an intermediary in numerous metabolic processes, including aerobic and anaerobic metabolism and as mediator of redox state among various compartments both within and between cells; however, its detailed function within these various "lactate shuttles" continues to be the subject of contemporary research.[31,32] Recent studies indicate that D-lactate is both metabolised to pyruvate by the enzyme D-α-hydroxy acid dehydrogenase and eliminated by the liver.[33] Additionally, the effect of lactate on physiological response continues to be more broadly studied. For example, it has been suggested that an increase in lactate concentration could upregulate vascular endothelial growth factor (VEGF) and potentially promote neovascularisation.[34] While these hypotheses remain unproven, they highlight the research interest surrounding lactate and its potentially efficacious effect on physiology.

Simple scaling arguments also put the physiological perturbation caused by the resorption of the scaffold in perspective. The naturally occurring level of L-lactate in the bloodstream is approximately 64.1 ± 8.0 mg/L at rest and can rise to levels as high as 810 ± 89 mg/L during exercise.[35] By contrast, the complete L-lactate degradation products from one 3.0 x 18 mm ABSORB Cohort B scaffold constitute 8.74 mg. Similarly, D-lactate is present in adult human blood serum in concentrations approximately 1 - 5% that of L-lactate (13-48 µmol/L, or alternatively, 1.16-4.27 mg/L) due to methylglyoxal metabolism,[36] whereas the amount created by the complete degradation of one 3.0 x 18 mm scaffold is 76 µg. Both quantities are quite small relative to the total amount of L- and D-lactate naturally present.

Nevertheless, it is important to evaluate the impact of the release of these species on tissue response. Figure 7 presents fractional polymer mass loss data from an in vivo study in the porcine model

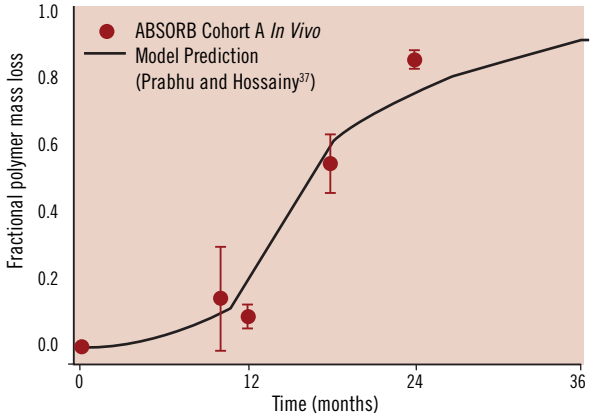

Figure 7. Fractional polymer mass loss data from the ABSORB Cohort A scaffold versus time in vivo in the porcine animal model. Sample sizes vary between n=3 and n=6. The curve represents the model of Prabhu and Hossainy.[37] Data are on file at Abbott Vascular.

for the ABSORB Cohort A scaffold. In this case, nearly 90% of the polymer mass was lost by the 24-month time point. However, in evaluating tissue response, it is more important to consider the time point at which the rate of mass loss is highest. To facilitate this assessment, the mass transport and reaction kinetics model of Prabhu and Hossainy[37] was employed to generate the solid line on Figure 7. The model predictions diverge at longer time points due to its assumption of constant volume and constant rate of reaction. Nevertheless, the model predicts that the highest rate of mass loss occurs between 12 and 15 months. If these degradation products were to elicit a tissue response, one would expect to observe it at a time point shortly thereafter. Hence, characteristic 12-month and 18-month histological slides taken from the left anterior descending artery are shown in Figure 8. The tissue exhibits modest neointimal thickening and low inflammation at both time points, suggesting that the maximum rate of mass loss associated with the implant does not cause a deleterious response.

Finally, it should be noted that the vasomotor function of the treated vessel is entirely natural throughout the resorption phase and beyond. That is not to say that vessel contraction and dilation will be possible in all patients despite the positive indications in the 2-year follow-up of the ABSORB Cohort A study.[9] Such a statement cannot be made when the range of patient physiologies and disease states is so diverse. Natural vasomotor function simply implies that the absence of scaffolding allows the vessel to respond to external stimuli if it is capable of doing so, similar to the theoretical response following PTCA.

Conclusions

The development of bioresorbable polymeric vascular scaffolds to fulfill the promise of VRT may give rise to a fourth revolution in PCI for the treatment of coronary artery disease. Vital to a successful device design concept is careful consideration of the physiological requirements. Design objectives are most clearly understood by dividing the scaffold lifetime into three phases: revascularisation, restoration, and resorption. The revascularisation phase is characterised by performance consistent with that of metallic DES. In the restoration phase, the characteristic time scales for lumen stabilisation and cellular matrix deposition are most relevant, as they dictate the duration the scaffold must provide radial scaffolding and the time point at which structural discontinuities are acceptable. Restoration of natural vascular response is theoretically possible when the scaffold has lost radial strength and structural continuity. In the resorption phase, the structurally discontinuous implant no longer serves any active role and is designed to be resorbed into the body in a benign fashion. As a result, the time point associated with the maximum rate of mass loss is potentially much more relevant scientifically and clinically than the time to full mass resorption. Future clinical studies will be critical to proving the hypotheses surrounding vasomotor and endothelial function in bioresorbable scaffolds.

References

1. Mintz GS, Popma JJ, Pichard AD, Kent KM, Satler LF, Wong C, Hong MK, Kovach JA, Leon MB. Arterial remodeling after coronary angioplasty: A serial intravascular ultrasound study. *Circulation* 1996;94:35-43.

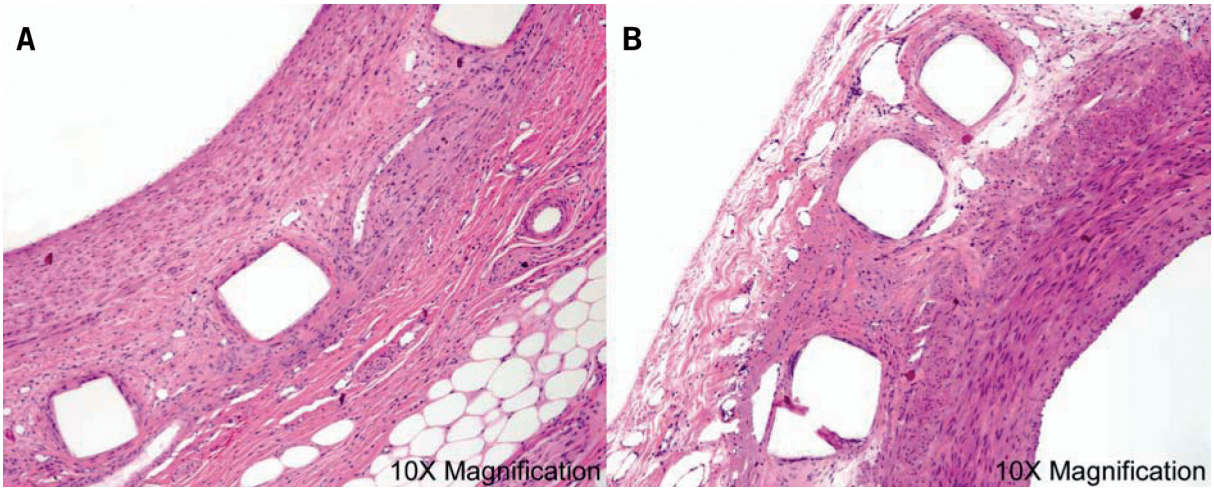

Figure 8. Histological slides of the (A) 12-month and (B) 18-month time points explanted from left anterior descending arteries of the porcine model. Data are on file at Abbott Vascular.

2. Serruys PW, Kutryk MJB, Ong ATL. Coronary-artery stents. *N. Engl. J. Med.* 2006;354:483-95.

3. Daemen J, Wenaweser P, Tsuchida K, Abrecht L, Vaina S, Morger C, Kukreja N, Jueni P, Sianos G, Hellige G, van Domburg RT, Hess OM, Boersma E, Meier B, Windecker S, Serruys PW. Early and late coronary stent thrombosis of sirolimus-eluting and paclitaxel-eluting stents in routine clinical practice: Data from a large two-institutional cohort study. *Lancet* 2007;369:667-78.

4. Finn AV, Joner M, Nakazawa G, Kolodgie F, Newell J, John MC, Gold HK, Virmani R. Pathological correlates of late drug-eluting stent thrombosis: Strut coverage as a marker of endothelialization. *Circulation* 2007;115:2435-41.

5. Kotani J-i, Awata M, Nanto S, Uematsu M, Oshima F, Minamiguchi H, Mintz GS, Nagata S. Incomplete neointimal coverage of sirolimus-eluting stents. Angioscopic findings. *J. Am. Coll. Cardiol.* 2006;47:2108-11.

6. Ormiston JA, Serruys PWS. Bioabsorbable coronary stents. *Circ.: Cardiovasc. Interventions* 2009;2:255-60.

7. Tamai H, Igaki K, Kyo E, Kosuga K, Kawashima A, Matsui S, Komori H, Tsuji T, Motohara S, Uehata H. Initial and 6-month results of biodegradable poly(L-lactic acid) coronary stents in humans. *Circulation* 2000;102:399-404.

8. Ormiston JA, Serruys PW, Regar E, Dudek D, Thuesen L, Webster MW, Onuma Y, Garcia-Garcia HM, McGreevy R, Veldhof S. A bioabsorbable everolimus-eluting coronary stent system for patients with single de-novo coronary artery lesions (ABSORB): A prospective open-label trial. *Lancet* 2008;371:899-907.

9. Serruys PW, Ormiston JA, Onuma Y, Regar E, Gonzalo N, Garcia-Garcia HM, Nieman K, Bruining N, Dorange C, Miquel-Hebert K, Veldhof S, Webster M, Thuesen L, Dudek D. A bioabsorbable everolimus-eluting coronary stent system (ABSORB): 2-year outcomes and results from multiple imaging methods. *Lancet* 2009;373:897-910.

10. Moncada S, Palmer RMJ, Higgs EA. Nitric oxide: physiology, pathophysiology, and pharmacology. *Pharmacol. Rev.* 1991;43:109-42.

11. Yanagisawa M, Kurihara H, Kimura S, Tomobe Y, Kobayashi M, Mitsui Y, Yazaki Y, Goto K, Masaki T. A novel potent vasoconstrictor peptide produced by vascular endothelial cells. *Nature* 1988;332:411-5.

12. Ludmer PL, Selwyn AP, Shook TL, Wayne RR, Mudge GH, Alexander RW, Ganz P. Paradoxical vasoconstriction induced by acetylcholine in atherosclerotic coronary arteries. *N. Engl. J. Med.* 1986;315:1046-51.

13. Gordon JB, Ganz P, Nabel EG, Fish RD, Zebede J, Mudge GH, Alexander RW, Selwyn AP. Atherosclerosis influences the vasomotor response of epicardial coronary arteries to exercise. *J. Clin. Invest.* 1989;83:1946-52.

14. Celermajer DS. Endothelial dysfunction: Does it matter? Is it reversible? *J. Am. Coll. Cardiol.* 1997;30:325-33.

15. Hambrecht R, Wolf A, Gielen S, Linke A, Hofer J, Erbs S, Schoene N, Schuler G. Effect of exercise on coronary endothelial function in patients with coronary artery disease. *N. Engl. J. Med.* 2000;342:454-60.

16. Pitt CG, Chasalow FI, Hibionada YM, Klimas DM, Schindler A. Aliphatic polyesters. I. The degradation of poly(ε-caprolactone) in vivo. *J. Appl. Polym. Sci.* 1981;26:3779-87.

17. Pitt CG, Gratzl MM, Kimmel GL, Surles J, Schindler A. Aliphatic polyesters. II. The degradation of poly(DL-lactide), poly(ε-caprolactone), and their copolymers in vivo. *Biomaterials* 1981;2:215-20.

18. Pitt CG, Gu ZW. Modification of the rates of chain cleavage of poly(ε-caprolactone) and related polyesters in the solid state. *J. Controlled Release* 1987;4:283-92.

19. Weir NA, Buchanan FJ, Orr JF, Dickson GR. Degradation of poly-L-lactide. Part 1: In vitro and in vivo physiological temperature degradation. *Proc. Inst. Mech. Eng., Part H* 2004;218:307-19.

20. Weir NA, Buchanan FJ, Orr JF, Farrar DF, Dickson GR. Degradation of poly-L-lactide. Part 2: Increased temperature accelerated degradation. *Proc. Inst. Mech. Eng., Part H* 2004;218:321-30.

21. Forrester JS, Fishbein M, Helfant R, Fagin J. A paradigm for restenosis based on cell biology: Clues for the development of new preventive therapies. *J. Am. Coll. Cardiol.* 1991;17:758-69.

22. Poncin P, Proft J. Stent Tubing: Understanding the Desired Attributes. Materials & Processes for Medical Devices, Anaheim, CA, 2003.

23. Ratner BD, Hoffman AS, Schoen FJ, Lemons JE, Editors. Biomaterials Science, An Introduction to Materials in Medicine. 2nd ed.; 2004.

24. Pennings AJ. Bundle-like nucleation and longitudinal growth of fibrillar polymer crystals from flowing solutions. *J. Polym. Sci., Polym. Symp.* 1977;59:55-86.

25. Kimata S, Sakurai T, Nozue Y, Kasahara T, Yamaguchi N, Karino T, Shibayama M, Kornfield JA. Molecular basis of the shish-kebab morphology in polymer crystallization. *Science* 2007;316:1014-7.

26. Kumaraswamy G, Kornfield JA, Yeh F, Hsiao BS. Shear-enhanced crystallization in isotactic polypropylene. 3. Evidence for a kinetic pathway to nucleation. *Macromolecules* 2002;35:1762-9.

27. Tadmor Z, Gogos CG. Principles of Polymer Processing. 2nd ed.; John Wiley & Sons, Inc.: Hoboken, NJ, 2006.

28. Serruys PW, Luijten HE, Beatt KJ, Geuskens R, de Feyter PJ, van den Brand M, Reiber JH, ten Katen HJ, van Es GA, Hugenholtz PG. Incidence of restenosis after successful coronary angioplasty: A time-related phenomenon. A quantitative angiographic study in 342 consecutive patients at 1, 2, 3, and 4 months. *Circulation* 1988;77:361-71.

29. Asakura M, Ueda Y, Nanto S, Hirayama A, Adachi T, Kitakaze M, Hori M, Kodama K. Remodeling of in-stent neointima, which became thinner and transparent over 3 years: serial angiographic and angioscopic follow-up. *Circulation* 1998;97:2003-6.

30. Holten CH, Mueller A, Rehbinder D. Lactic Acid - Properties and Chemistry of Lactic Acid and Derivatives. Verlag Chemie: Weinheim, 1971.

31. Gladden LB. Lactate metabolism: A new paradigm for the third millennium. *J. Physiol.* 2004;558:5-30.

32. Philp A, MacDonald AL, Watt PW. Lactate - A signal coordinating cell and systemic function. *J. Exp. Biol.* 2005;208:4561-75.

33. Ewaschuk JB, Naylor JM, Zello GA. D-Lactate in human and ruminant metabolism. *J. Nutr.* 2005;135:1619-25.

34. Constant JS, Feng JJ, Zabel DD, Yuan H, Suh DY, Scheuenstuhl H, Hunt TK, Hussain MZ. Lactate elicits vascular endothelial growth factor from macrophages: A possible alternative to hypoxia. *Wound Repair Regen.* 2000;8:353-60.

35. Stanley WC, Gertz EW, Wisneski JA, Morris DL, Neese RA, Brooks GA. Systemic lactate kinetics during graded exercise in man. *Am. J. Physiol.* 1985;249:E595-E602.

36. McLellan AC, Phillips SA, Thornalley PJ. Fluorometric assay of D-lactate. *Anal. Biochem.* 1992;206:12-6.

37. Prabhu S, Hossainy S. Modeling of degradation and drug release from a biodegradable stent coating. *J. Biomed. Mater. Res.,* Part A 2007;80A:732-41.